

Effects of lithium nitrate admixture on early-age cement hydration

M.J. Millard¹, K.E. Kurtis^{*}

School of Civil and Environmental Engineering, Georgia Institute of Technology, 790 Atlantic Dr., Atlanta, GA 30332, USA

Received 11 June 2007; accepted 20 November 2007

Abstract

Although the benefits of lithium admixtures for mitigation of alkali–silica reaction (ASR) have been well documented, the potential ancillary effects of lithium compounds on cement and concrete remain largely uncharacterized. To examine the effects of the most common lithium admixture — lithium nitrate — on early-age behavior, the admixture was introduced at dosages of 0% to 400% of the recommended dosage to six cements of varying composition and to a cement-fly ash blend. Behavior was examined by isothermal calorimetry and measurements of chemical shrinkage, autogenous shrinkage, and setting time. Results indicate that lithium nitrate accelerates the early hydration of most cements but may retard hydration after 24 h. In the lowest alkali cement tested, set times were shortened in the presence of lithium nitrate by 15–22%. Higher dosages appeared to increase autogenous shrinkage after 40 days. The replacement of cement by Class F fly ash at 20% by weight appeared to diminish the early acceleration effects, but later hydration retardation and autogenous shrinkage were still observed.

© 2007 Elsevier Ltd. All rights reserved.

Keywords: Acceleration; Alkalies; Lithium compounds; Setting; Shrinkage

1. Introduction

Since its identification [1], alkali–silica reaction (ASR) has been observed in many structures across the United States and the rest of the world [2–4]. The concrete cracking that is caused by ASR can lead to reduced stiffness and increased permeability in concrete structures. ASR damage has typically been observed in pavements, bridges, dams, and other structures exposed to moisture over several decades. However, recently ASR-induced damage has been identified at earlier ages (10 years of age and younger) in concrete airfield pavements in Atlanta, St. Louis, Memphis, Denver, Colorado Springs, Salt Lake City, Detroit, and at Mountain Home Air Force Base and Andrews Air Force Base, among others. In addition to increased permeability and decreased stiffness, progressive ASR cracking in airfield pavements can lead to “foreign object debris” (FOD), a significant hazard to aircraft. Recent research [5] has linked the early onset of ASR damage

observed in airfield pavements to alkali-based de-icing chemicals, introduced for use at airfields in the 1990s.

In response to recent ASR damage, lithium-containing admixtures are increasingly being specified for airfield pavements and other types of construction where de-icing chemicals are used. Recent lithium admixture use includes airfield pavement construction at Hartsfield-Jackson Atlanta International Airport (H-JAIA) as well as in bridge and highway construction in New Mexico, Texas, South Dakota, Pennsylvania, and Delaware [3].

Since the discovery of the beneficial effects of lithium compounds for ASR mitigation [6], most related research has focused on determining optimal compounds and dosages of lithium to suppress ASR-related expansion. Other effects on cement and concrete behavior have not been previously examined in a comprehensive manner.

There is interest in using lithium nitrate admixtures at lower than usual dosages (for economy and for control of marginally reactive aggregate) and at higher than usual dosage rates in an attempt to provide additional or longer term protection from ASR damage. However, the ancillary effects of these larger dosage rates — as with the effects of the recommended dosage rate — on concrete behavior have not been the subject of prior comprehensive investigation. The purpose of this research is to examine any

^{*} Corresponding author. Tel.: +1 404 385 0825; fax: +1 404 894 0211.

E-mail addresses: mmillard@sedkiruss.com (M.J. Millard),
kkurtis@ce.gatech.edu (K.E. Kurtis).

¹ Fax: +1 404 894 0211.

potential effects of a range of lithium admixture dosages on early-age behavior.

2. Experimental program

2.1. Materials

Lithium nitrate (LiNO_3) was selected for this research because it is currently the most commonly used lithium compound for ASR suppression. Previous research has established that the lithium nitrate dosage required for effective ASR suppression is a function of the total alkali content of the cement used. A dosage of 0.74 lithium-to-alkali molar ratio has generally been found effective for suppression of ASR [3,7–9], and this dosage is recommended by the manufacturer. In this study, the dosage of admixture providing this 0.74 lithium-to-alkali molar ratio for each cement is labeled the “100% dosage” for that cement.

To identify any upper lithium dosage limit, above which negative effects may occur, the behavior of mixtures was examined at several lithium nitrate dosages, up to 400% of the standard effective dosage. Interest exists in using lithium admixtures at higher dosages to potentially provide additional or longer term protection against damage and to potentially offset the adsorption of the admixture into hydration products and loss by leaching.

Prior research on lithium hydroxide used as an ASR-mitigating admixture [10] suggested that the alkali content of the cement may influence ancillary effects of lithium in concrete mixtures, while anecdotal evidence suggested a link with cement tricalcium aluminate (C_3A) content. Thus, six cements of varying alkali and tricalcium aluminate (C_3A) contents were selected for this investigation. Oxide compositions of these cements are summarized in Table 1. Cement 6, which was used

in recent construction with lithium admixtures at Hartsfield-Jackson Atlanta International Airport, was examined both with and without 20% Class F fly ash replacement.

Prior to mixing, all materials and tools were conditioned at 25 °C in an environmental chamber for 48 h.

2.2. Methods

2.2.1. Heat of hydration

Paste batches of 0.45 lb (204 g) were mixed at a water-to-cementitious materials ratio (w/cm) of 0.30. This w/cm ratio was selected to mimic typical concrete mixes used for airfield pavements. After mixing, paste quantities of approximately 5 g each were placed in 20 ml plastic ampoules, which were maintained at a temperature of 25 °C in a 3114 TAM Air Isothermal Calorimeter. Heat generation data were recorded every 60 s for 72 h for each paste specimen.

2.2.2. Chemical shrinkage

Chemical shrinkage of pastes was measured following ASTM C 1608-05, the Standard Test Method for Chemical Shrinkage of Hydraulic Cement Paste [11]. Pastes were mixed at a w/cm of 0.40 (higher than in other testing in this research). This higher w/cm ratio, specified by ASTM 1608, is necessary to allow water migration through the paste. Each 5-g specimen was vibrated in a glass vial, and de-aerated water was added carefully to cover the paste. Rather than filling the vial with water as ASTM C 1608-05 prescribes, cover water was limited to 3 g to minimize any leaching of lithium ions from the paste into the water. This was the only significant deviation from the ASTM C 1608-05 procedure. The remainder of the vial was filled with hydraulic oil. The vial was then sealed with a rubber

Table 1
Oxide analysis and Bogue potential compositions for cements and fly ash

	Cement 1 Low alkali	Cement 2 Moderate alkali and C_3A	Cement 3 High alkali	Cement 4 Low C_3A	Cement 5 High C_3A	Cement 6	Class F fly ash
SiO_2 (%)	20.44	20.98	20.13	21.00	19.29	20.06	50.77
Al_2O_3 (%)	5.24	4.72	5.48	3.62	5.62	4.89	19
Fe_2O_3 (%)	3.99	2.99	3.26	3.47	2.82	3.00	17.72
CaO (%)	63.22	63.56	60.93	62.52	64.21	64.22	5.1
MgO (%)	1.05	2.24	2.45	4.29	0.86	2.68	0.91
SO_3 (%)	3.74	2.61	4.00	2.43	3.54	2.74	1.56
Na_2O (%)	0.069	0.165	0.344	0.231	0.257	0.115	0.65
K_2O (%)	0.343	0.523	0.866	0.404	0.464	0.444	2.31
Na_2O equiv. (%)	0.295	0.509	0.91	0.50	0.562	0.407	2.17
P_2O_5 (%)	0.092	0.335	0.157	0.054	0.256	0.076	0.12
TiO_2 (%)	0.318	0.241	0.214	0.172	0.614	0.274	1.08
SrO (%)	0.065	0.035	0.194	0.050	0.231	0.038	0.04
Mn_2O_3 (%)	0.079	0.150	0.173	0.064	0.040	0.088	0.05
Cr_2O_3 (%)	0.012	0.008	0.025	0.005	0.014	0.012	–
LOI (%)	1.33	1.44	1.78	1.69	1.79	1.37	0.62
C_3S (%)	50.4	55.9	42	59	62.9	64.1	NA
C_2S (%)	20.6	18.0	26	16	7.9	9.2	NA
C_3A (%)	7.1	7.5	9	4	10.1	7.9	NA
C_4AF (%)	12.2	9.1	10	11	8.6	9.1	NA
Blaine fineness, (m^2/kg)	380	369	376	370	368	345	161

stopper with a 1.0 ml pipette inserted through it. Subsequent volume changes were measured by reading the oil level on gradations of the pipette for 28 days. Specimens were kept in an environmental chamber for the duration of the test, with observed temperatures within a range of 24.5 ± 0.4 °C.

2.2.3. Vicat time of setting

Time of setting was measured for pastes following ASTM C 191-04b Standard Test Method for Time of Setting of Hydraulic Cement by Vicat Needle [12]. Paste batches of 7 lb (3.175 kg) were mixed at a w/cm of 0.30, following ASTM C 305-99 Standard Practice for Mechanical Mixing of Hydraulic Cement Pastes and Mortars of Plastic Consistency [13]. Triplicate specimens for each mix were molded and sealed in plastic containers containing wet aggregate to provide temperature stability and humidity. The specimens were periodically tested to determine initial (i.e., Vicat needle penetration of 25 mm) and final set. Ambient temperature was approximately 25 °C.

In order to simulate worst case field conditions, Vicat time of setting was also measured at 35 °C. For these elevated temperature tests, Cement 6 was examined both with and without 20% Class F fly ash replacement, at 0% to 400% LiNO_3 dosages. Materials and the sealed humid containers were preconditioned in an oven at 35 °C for 24 h preceding the testing, and remained in the oven between periodic penetration measurements.

2.2.4. Autogenous shrinkage

A method similar to that described by Jensen and Hansen (1995) [14] was used to measure autogenous shrinkage. Cement paste specimens were sealed in flexible corrugated plastic tubes that allow linear deformation with minimal resistance. Jensen and Hansen controlled specimen temperature in a glycol bath while recording length changes using an automatic data logger. In this research, specimens were kept in an environmental chamber between periodic manual measurements using a dilatometer.

Autogenous shrinkage specimens were made from the same paste batches as the Vicat time of setting specimens. Initial specimen length measurements were taken when the Vicat specimens reached final set. For the subsequent 100 days of measurements, temperatures in the environmental chambers were observed to fluctuate within a range of 24.5 ± 0.4 °C.

3. Results and discussion

3.1. Heat of hydration

In general, as the dosage of lithium nitrate increased, the early hydration reactions were accelerated. This is apparent in the heat of hydration curves in Figs. 1–6. At increasing admixture dosages, the curves generally shift upward and to the left. Figs. 1–3 illustrate the effects of lithium nitrate on Cements 1, 2, and 3 (the low, moderate, and high alkali cements). Fig. 1 illustrates earlier heat generation for each increase in lithium nitrate dosage in the low alkali cement. However, data for the moderate and high alkali Cements 2 and 3, in Figs. 2 and 3, suggest that above some level of lithium dosage, further accel-

eration does not occur. For example, in the high alkali Cement 3 in Fig. 3, the 50% dosage appears to increase the early heat of reaction, but no further increases are apparent above the 50% lithium dosage (corresponding to 1.5 gal/yd³ or 7.4 l/m³ for a typical airfield pavement mix). In the moderate alkali Cement 2 in Fig. 2, no further increases are apparent above 200% dosage (corresponding to 3.4 gal/yd³ or 16.8 l/m³). The low alkali Cement 1 shows continued heat increases up to the highest level tested, 400% dosage (corresponding to 4 gal/yd³ or 19.8 l/m³). The low alkali cement was accelerated by each incremental dosage increase, but the higher alkali cements did not show further acceleration by higher dosages. These results suggest that lower alkali cements are more susceptible to greater heat evolution increases due to the addition of this lithium admixture.

Bentz [15] also observed acceleratory effects of lithium, and concluded that they are similar to the acceleratory effects of potassium and sodium; all three are Group I alkali elements, with 1 valence shell electron. Potassium and sodium ions from the cement (or added as soluble salts) reduce the solubility of calcium ions. This promotes the nucleation of the calcium-containing hydration products [16]. The acceleratory period of the hydration of tricalcium silicate (C_3S) is likely governed by this nucleation [17]. Hydration acceleration by LiNO_3 observed in this study suggests that lithium ions may have similar effects on the solubility of calcium ions in solution, on the nucleation of calcium-containing hydration products, and on C_3S hydration acceleration.

The upper limit on the acceleratory effects of increasing dosages of lithium nitrate shown in Figs. 2 and 3 suggests that above some lithium ion concentration, increases in lithium concentration have diminishing effects on nucleation of hydration products. Since this upper threshold is apparently reached at a lower lithium dosage in the high alkali cement, it is likely that nucleation is affected by the combined alkali ion concentration: $[\text{Li}^+ + \text{Na}^+ + \text{K}^+]$. At some level of total alkali ion concentration, a maximum early heat generation profile is reached. It is proposed that this alkali ion concentration is reached at lower lithium dosages for high alkali cements, because the total alkali concentration is already very high due to the contribution of the cement alkalis (Na^+ and K^+). *Of significance in this observation is that the cements which are most vulnerable to hydration acceleration are also the cements that are most likely to be combined with lithium admixture in practice.* That is, low alkali cements, which are typically specified in applications where ASR is a consideration, appear to be accelerated more by LiNO_3 .

Figs. 4 and 5 illustrate the heat of hydration effects of lithium nitrate on Cements 4 and 5, respectively (the low and high C_3A cements). The data in Fig. 4 for the low C_3A Cement 4 show an approximate 3 h shift to the left due to the higher LiNO_3 dosages, indicating a significantly earlier hydration period. However, the data for the high C_3A Cement 5 in Fig. 5 show only a very subtle shift (less than 1 h) to the left at increasing dosages. This suggests that lithium nitrate may accelerate lower C_3A cements more than higher C_3A cements.

In addition to the aforementioned acceleration of the C_3S reactions, lithium nitrate appeared to accelerate the C_3A reactions in some cases. This acceleration, most apparent in the moderate

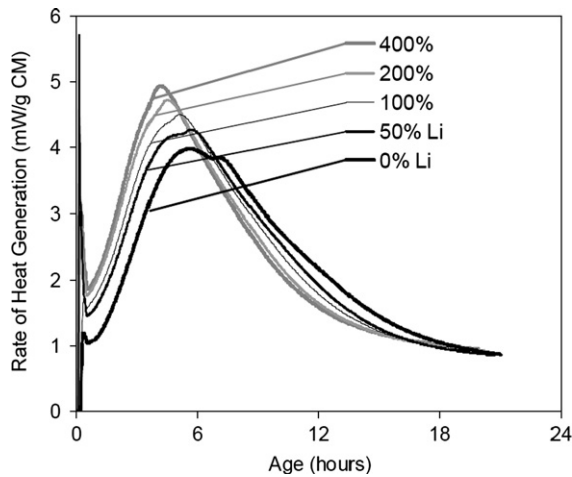


Fig. 1. Calorimetry results for Cement 1 (low alkali cement) at increasing LiNO₃ dosages.

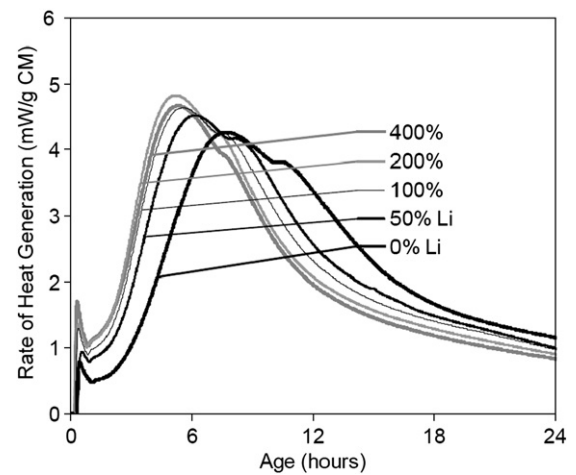


Fig. 4. Calorimetry results for Cement 4 (low C₃A cement) at increasing LiNO₃ dosages.

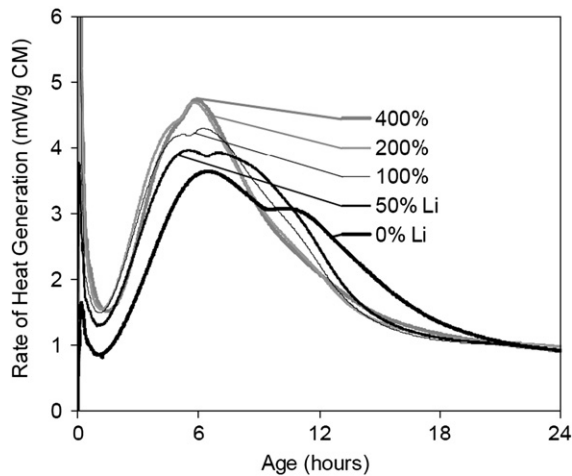


Fig. 2. Calorimetry results for Cement 2 (moderate alkali/moderate C₃A cement) at increasing LiNO₃ dosages.

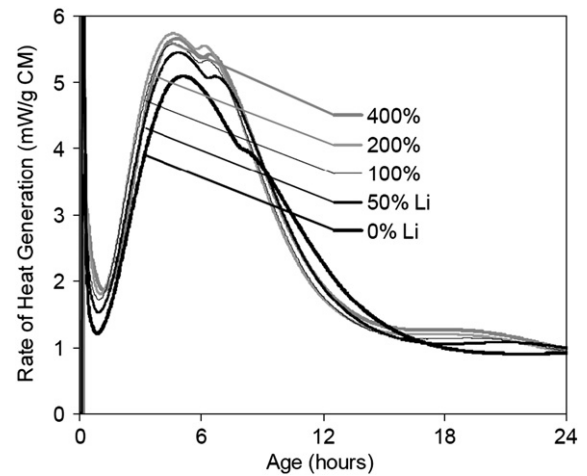


Fig. 5. Calorimetry results for Cement 5 (high C₃A cement) at increasing LiNO₃ dosages.

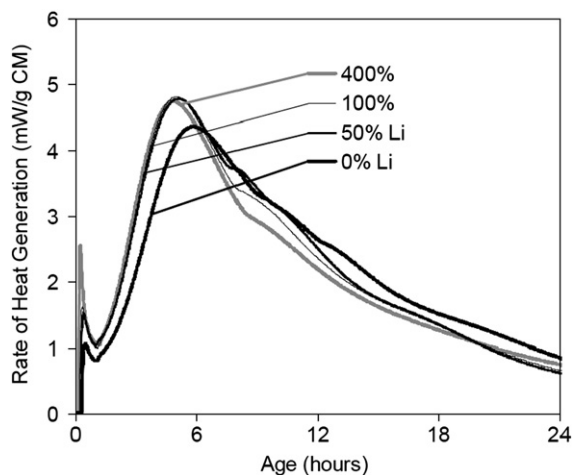


Fig. 3. Calorimetry results for Cement 3 (high alkali cement) at increasing LiNO₃ dosages.

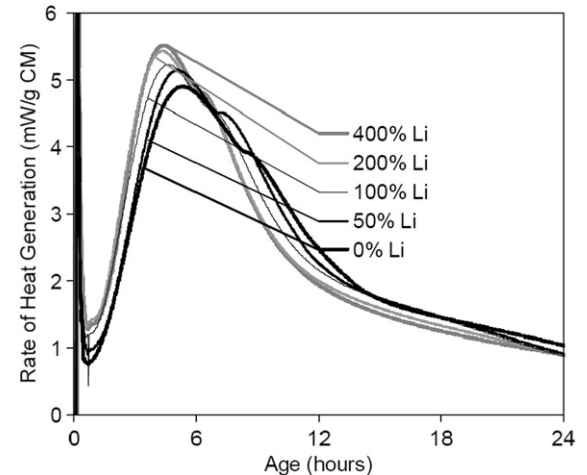


Fig. 6. Calorimetry results for Cement 6 without fly ash, at increasing LiNO₃ dosages.

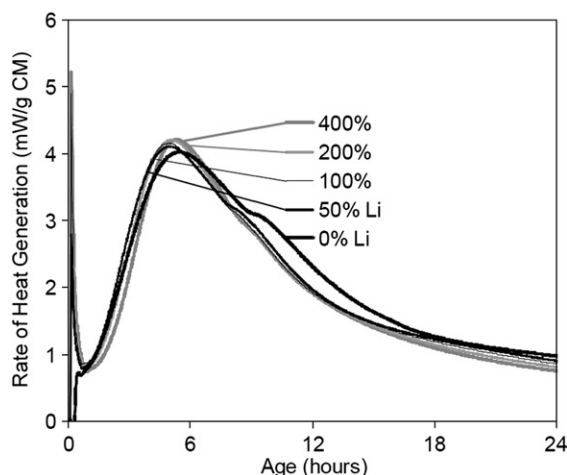


Fig. 7. Calorimetry results for Cement 6 with 20% fly ash replacement, at increasing LiNO_3 dosages.

alkali/moderate C_3A Cement 2 in Fig. 2, is indicated by a change in the overall shape of the heat generation profile. The second “hump” of the heat generation profile (the hump occurring at approximately 11 h for the control case with no lithium) appears to shift to the left slightly more than the overall profile. This second hump is generally attributed to reactions of the C_3A component of the cement. The control mix curve in Fig. 2 shows a 4 to 6 h delay between the initial reaction (C_3S) peak and the secondary (C_3A) peak. The 50% lithium nitrate dosage curve for the same cement, however, shows only an approximate 2-h delay. At progressively higher lithium nitrate dosages, the C_3A peak shifts left relative to the C_3S peak, so that at the 400% dosage, the two peaks are nearly aligned. This behavior is also clearly visible in the Cement 1 curves in Fig. 1, but is less evident in the other cements. This behavior may be related to effects of lithium on the rate of C_3A dissolution. Alkalies (sodium and potassium) have been shown to promote the dissolution of C_3A , accelerating subsequent reactions [16]. Alkalies often, based on this behavior, serve as set accelerators in commercial applications [18]. Figs. 1 and 2

suggest that lithium, also a Group I alkali element, may similarly promote C_3A dissolution, and accelerate C_3A hydration. Although C_3A reaction acceleration can have unwanted effects on workability, time of setting, shrinkage, and strength, none of these effects were observed in this research.

Figs. 6 and 7 show results of calorimetry tests on Cement 6 alone and with 20% Class F fly ash replacement. In these plots, rate of heat generation is reported as milliwatts per gram of cementitious material (including the fly ash). As expected, at a constant w/cm of 0.30, lower heats were generated with the 20% fly ash replacement than with the cement alone. Acceleration of Cement 6 hydration without fly ash is consistent with behaviors observed in Figs. 1–5. However, effects on heat of hydration are clearly less significant with the Class F fly ash in Fig. 7. This suggests that Class F fly ash replacement may decrease the (possibly undesirable) effects of lithium nitrate on early heat of hydration. This observation is relevant because Class F fly ash, due to its ASR-mitigating effects, is likely to be used in lithium-containing mixes.

Previous research has found that some lithium ions in the mix water become bound in the structure of the hydrated cement. Lithium ions apparently replace some of the calcium ions in the formation of calcium silicate hydrate (C–S–H) [19]. The reduced calcium-to-silica ratio of the C–S–H in a Class F fly ash mix increases this lithium binding. It is proposed that the subsequent lower concentration of lithium in the pore solution contributes to the observation of less acceleration in mixes containing Class F fly ash and lithium nitrate.

Figs. 8 and 9 show longer-duration cumulative heat evolution for Cement 6 with and without 20% fly ash replacement. Cumulative heat in these plots is measured in joules per gram of cementitious material, and is equal to the area under the curves in Figs. 6 and 7. In both figures, cumulative heat curves for the control (no lithium) case exceed that for the 400% dosage case after 1 day. Although lithium-dosed pastes generated more heat initially, cumulative heat curves after 1 day are lower than those for the control mixes. This may indicate that hydration after 24 h is retarded by higher lithium dosages. Unlike the early heat

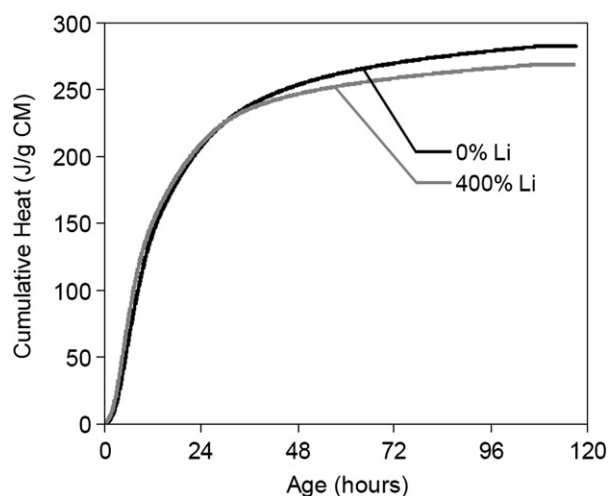


Fig. 8. Cumulative heat generation for Cement 6 without fly ash.

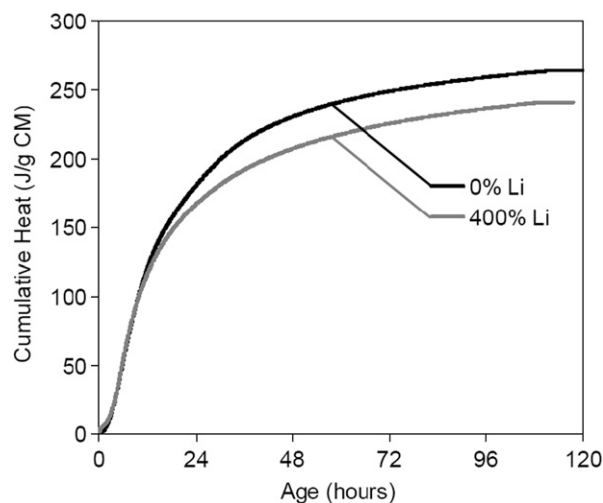
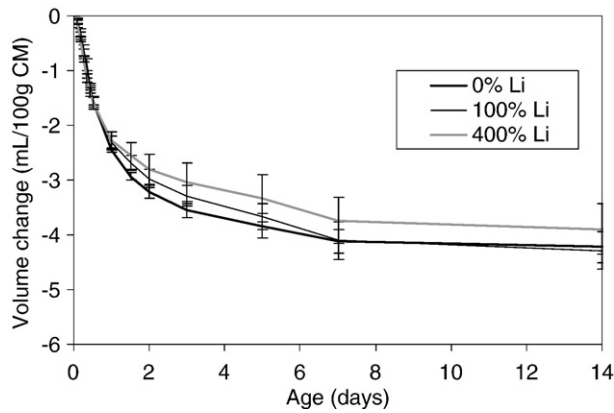
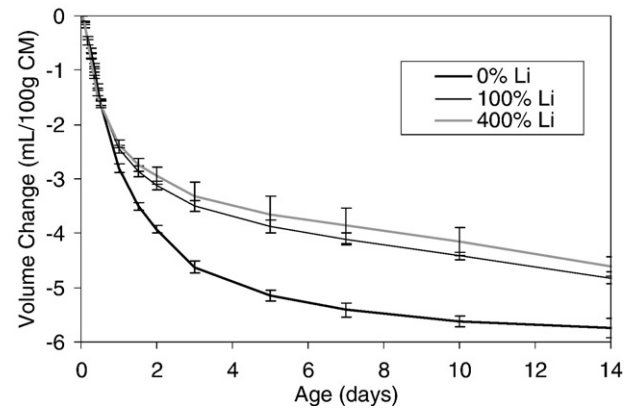
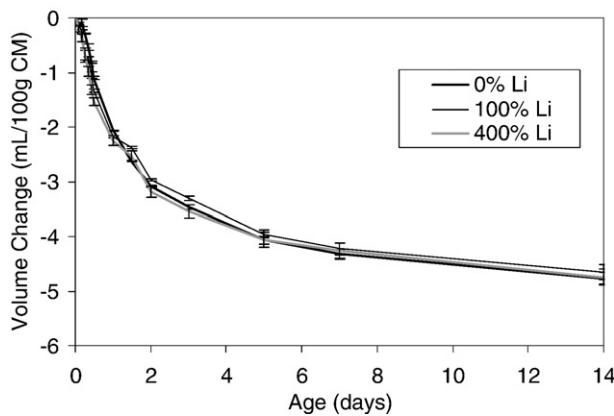
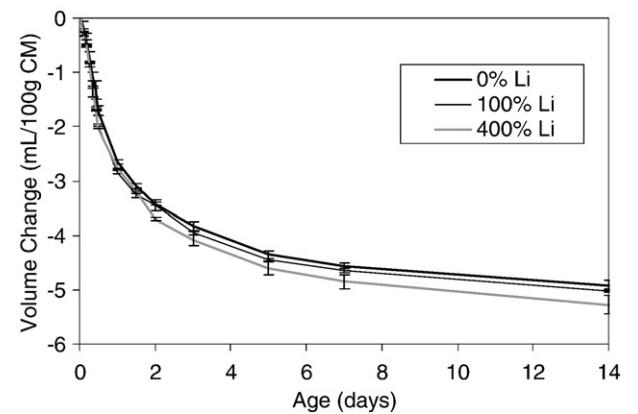


Fig. 9. Cumulative heat generation for Cement 6 with 20% fly ash replacement.

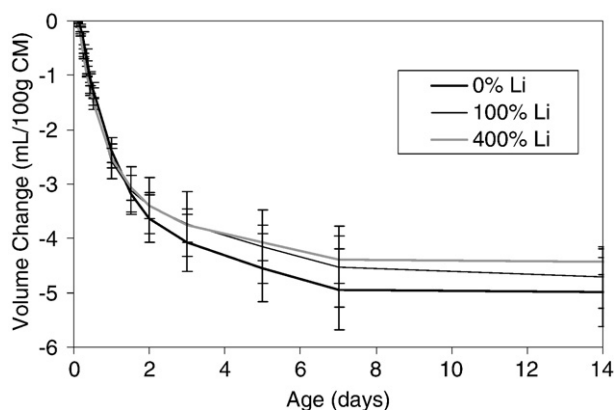
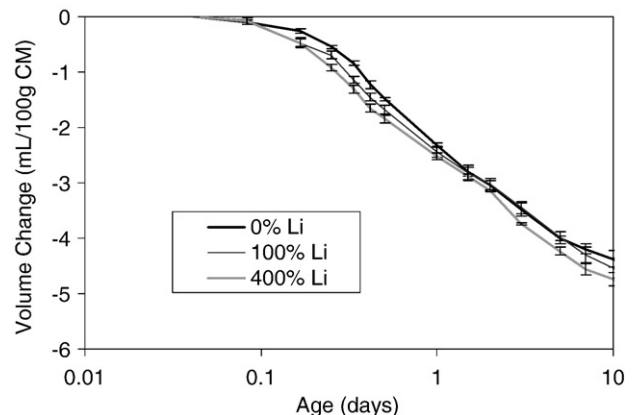
Fig. 10. Chemical shrinkage for Cement 1 at increasing LiNO_3 dosages.Fig. 13. Chemical shrinkage for Cement 4 at increasing LiNO_3 dosages.Fig. 11. Chemical shrinkage for Cement 2 at increasing LiNO_3 dosages.Fig. 14. Chemical shrinkage for Cement 5 at increasing LiNO_3 dosages.

generation effects of lithium, this lower cumulative heat effect occurs with or without the 20% fly ash replacement.

3.2. Chemical shrinkage

Chemical shrinkage, the absolute volume change of a hydrating cement, is approximately proportional to the extent of hydration [11]. As expected, results for chemical shrinkage on cement pastes in Figs. 10–16 show trends similar to those obtained by

calorimetry. Cements 1, 2, 3, and 5 showed greater shrinkage in the first 24 h of hydration with increasing lithium admixture dosage, presumably due to greater extent of reaction as indicated by calorimetry. The delay of chemical shrinkage in the control mixes in these cements was indicative of the later hydration of these control mixes. Higher lithium nitrate dosages showed chemical shrinkage earlier, indicating hydration acceleration. The hydration acceleration in this data is less apparent than in the

Fig. 12. Chemical shrinkage for Cement 3 at increasing LiNO_3 dosages.Fig. 15. Chemical shrinkage for Cement 6 without fly ash, at increasing LiNO_3 dosages (semi-logarithmic plot).

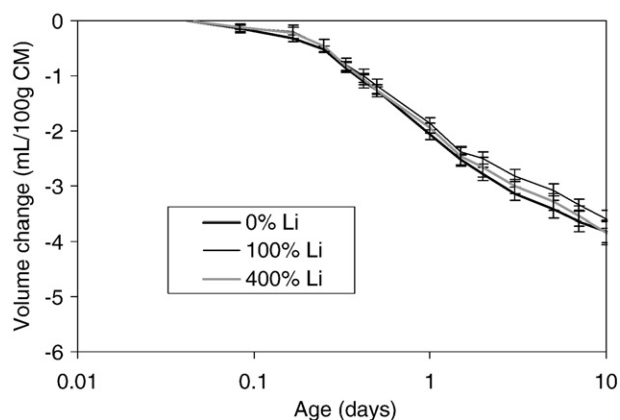


Fig. 16. Chemical shrinkage for Cement 6 with 20% fly ash replacement, at increasing LiNO_3 dosages (semi-logarithmic plot).

calorimetry data, but it does in some cases corroborate the acceleratory effect of lithium nitrate on hydration in the first 24 h.

Control samples for Cements 1, 3, and 4, in Figs. 10, 12, and 13 respectively, show greater chemical shrinkage than the lithium-containing pastes after 24 h. This corresponds to the trends observed in Figs. 8 and 9. That is, although the lithium-dosed mixes hydrate faster initially, hydration may be retarded after 1 day.

Figs. 15 and 16 illustrate the effect of lithium nitrate dosage on chemical shrinkage for Cement 6 alone and with fly ash. This data is plotted semi-logarithmically in order to better examine the first 24 h of hydration. In Fig. 15, chemical shrinkage in the first 24 h is greater in lithium-dosed mixes. This suggests that lithium nitrate dosages accelerate early chemical shrinkage (and hydration). Fig. 16 does not show this lithium nitrate effect on early chemical shrinkage in fly ash-containing specimens. This

agrees with calorimetry observations that fly ash may decrease the early acceleratory effects of lithium nitrate.

3.3. Time of setting

Tables 2 and 3 show results from Vicat time of setting testing. Of the seven cement cases tested, the only cement to show a clear setting time dependency on lithium dosage was the low alkali Cement 1, with a Na_2O_e of 0.295%. In the Cement 1 tests, the standard dosage of lithium nitrate decreased the initial setting time by 15%, and the final setting time by 22%. The 400% dosage decreased initial and final setting times by 25% and 32%, respectively. As expected, Table 3 indicates that longer setting times were observed with the use of fly ash. However, no clear effect of lithium nitrate was observed in Cement 6 with or without fly ash replacement. Table 3 also indicates that in tests of Cement 6 with and without fly ash at an elevated temperature of 35 °C to simulate more extreme field conditions, no LiNO_3 effects on set time were apparent at any dosage.

Based on the acceleration of cement hydration observed in calorimetry and chemical shrinkage testing, LiNO_3 may be expected to shorten setting times in some cements. Shortened setting times have been reported for cement-based materials containing other lithium compounds (LiCO_3 and LiOH) [20,21]. However, with the exception of the lowest alkali cement, LiNO_3 showed no influence on the setting times of the cements tested. Thomas et al. [22] also found no consistent and discernible effect of LiNO_3 on setting time in fly ash-containing pastes. It may be significant that the only cement where the setting time was apparently affected by the lithium nitrate admixture is the lowest alkali cement. The calorimetry results also suggested that lower alkali cements are more susceptible to hydration reaction acceleration. The lithium sensitivity of a cement likely depends

Table 2
Vicat initial and final set times (with standard deviations) for pastes of Cements 1–5 at increasing LiNO_3 dosages

Li dosage	Cement 1 setting times, min		Cement 2 setting times, min		Cement 3 setting times, min		Cement 4 setting times, min		Cement 5 setting times, min	
	Initial	Final	Initial	Final	Initial	Final	Initial	Final	Initial	Final
0%	140 (2)	316 (22)	148 (4)	328 (13)	164 (7)	337 (7)	184 (1)	344 (10)	98 (6)	223 (14)
100%	118 (4)	247 (6)	123 (2)	231 (8)	144 (3)	273 (6)	154 (3)	322 (13)	92 (0)	208 (0)
400%	104 (2)	214 (5)	140 (6)	305 (5)	181 (2)	361 (10)	156 (2)	319 (18)	111 (2)	236 (17)

Table 3
Vicat initial and final set times (with standard deviation) for Cement 6 pastes, with and without 20% fly ash replacement, cured at 25 °C and at 35 °C

Li dosage	Cured at 25 °C				Cured at 35 °C			
	Cement 6 setting times, min		Cement 6 with 20% fly ash setting times, min		Cement 6 setting times, min		Cement 6 with 20% fly ash setting times, min	
	Initial	Final	Initial	Final	Initial	Final	Initial	Final
0%	121 (2)	237 (15)	141 (2)	289 (23)	98 (1)	223 (19)	112 (1)	238 (0)
50%	86 (12)	206 (9)	161 (8)	329 (6)	114 (7)	204 (19)	142 (3)	250 (4)
100%	102 (0)	221 (31)	148 (3)	331 (8)	91 (2)	189 (7)	125 (0)	230 (12)
200%	99 (2)	201 (18)	161 (2)	258 (16)	97 (1)	189 (0)	140 (1)	238 (12)
400%	117 (3)	218 (0)	179 (11)	328 (13)	102 (2)	214 (9)	121 (3)	230 (9)

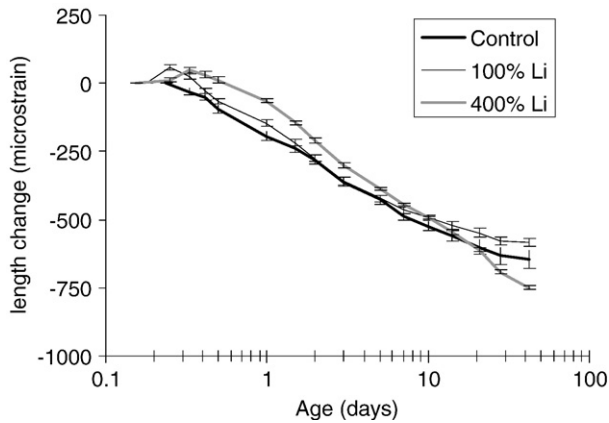


Fig. 17. Autogenous shrinkage of Cement 1 specimens at increasing LiNO_3 dosages (semi-logarithmic plot).

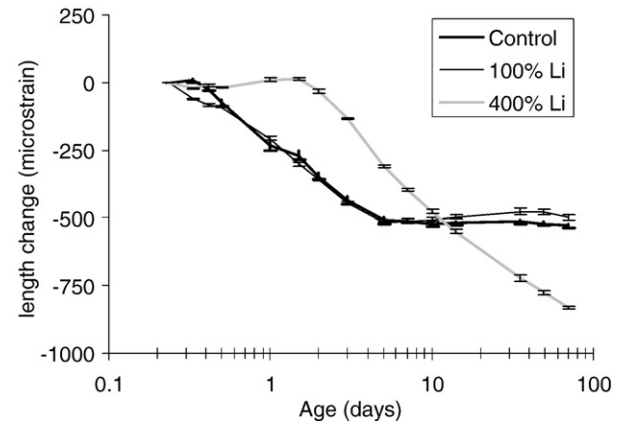


Fig. 20. Autogenous shrinkage of Cement 4 specimens at increasing LiNO_3 dosages (semi-logarithmic plot).

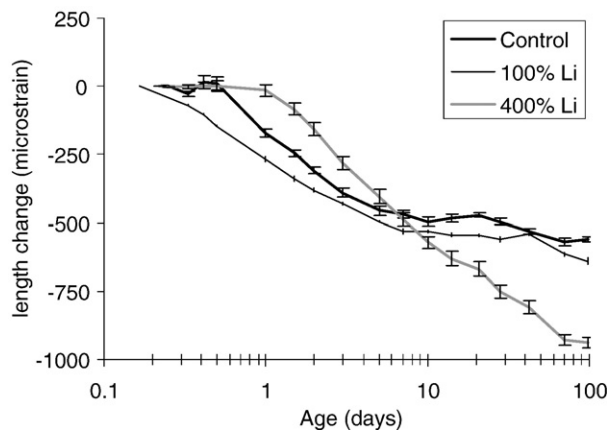


Fig. 18. Autogenous shrinkage of Cement 2 specimens at increasing LiNO_3 dosages (semi-logarithmic plot).

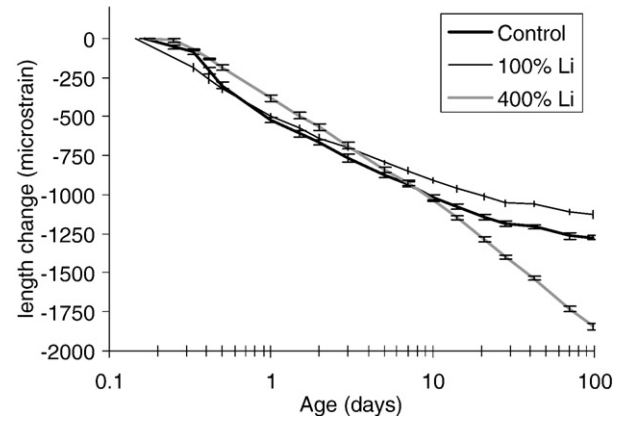


Fig. 21. Autogenous shrinkage of Cement 5 specimens at increasing LiNO_3 dosages (semi-logarithmic plot).

on more variables than alkali content alone, but it is proposed that cement alkali content is a key factor.

Also of significance in these results is that although calorimetry suggested acceleration of the C_3A reactions, behaviors sometimes associated with C_3A acceleration were not observed in time of

setting tests at lithium dosages up to 400%. That is, no indications of early stiffening or flash-set were observed at any dosage.

3.4. Autogenous shrinkage

Linear deformation due to autogenous shrinkage was measured in cement pastes cast in sealed, corrugated polymeric

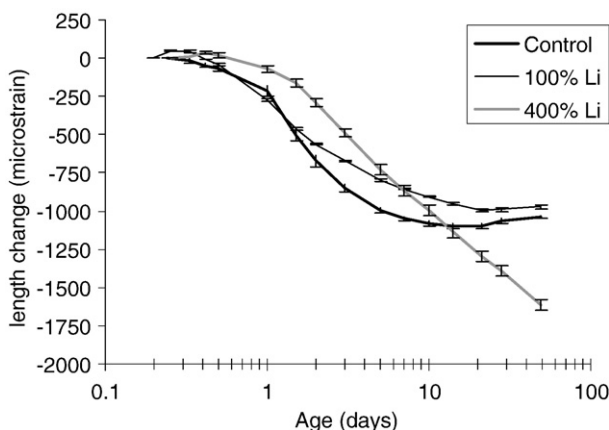


Fig. 19. Autogenous shrinkage of Cement 3 specimens at increasing LiNO_3 dosages (semi-logarithmic plot).

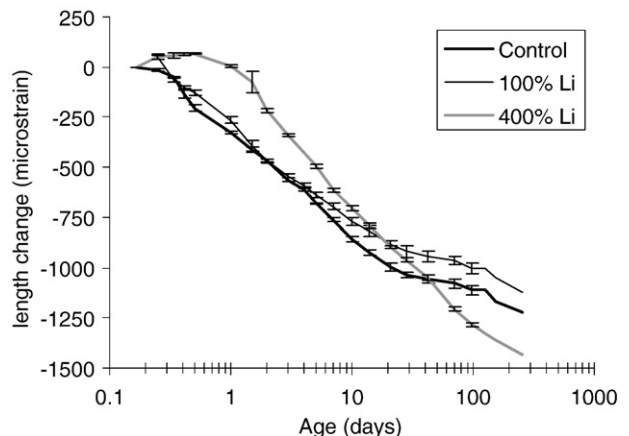


Fig. 22. Autogenous shrinkage of Cement 6 specimens at increasing LiNO_3 dosages (semi-logarithmic plot).

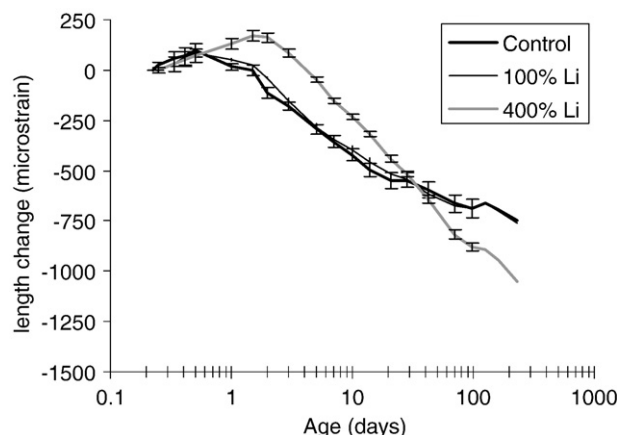


Fig. 23. Autogenous shrinkage of Cement 6 specimens with 20% fly ash replacement at increasing LiNO_3 dosages (semi-logarithmic plot).

tubes by the method described by Jensen and Hansen [13] (1995). While chemical shrinkage is an absolute volume change from the time of mixing, autogenous shrinkage is a measured linear deformation, measured after final setting, and is largely due to self-desiccation in the capillary pores of the developing hydrated cement microstructure [13,23].

Effects of lithium nitrate dosages on autogenous shrinkage were examined in all six cements, as well as the additional case of Cement 6 with fly ash replacement. Results are illustrated in Figs. 17–23. Generally, as the lithium dosage increased, less autogenous shrinkage was observed in the first 10 days. Often, a net expansion occurred in the first 24 h. In particular, Cement 4 in Fig. 20 shows expansion at the 400% lithium dosage and shrinkage at 0% and 100% dosage.

After 28 days, pastes with the highest (400%) dosages exhibited significantly greater autogenous shrinkage than the control samples. However, in all conditions examined, pastes produced with the standard dosage of lithium nitrate (100% dosage) did not exhibit significantly more autogenous shrinkage than the corresponding control (no lithium) mixes.

Comparison of data for autogenous shrinkage in the Cement 6 pastes prepared with and without fly ash (Figs. 22 and 23) shows no clear influence of fly ash replacement on the lithium effects on autogenous shrinkage. Overall shrinkage appears less in the fly ash mixes when compared to the cement alone, but the effects of lithium appear the same in both. Both with and without fly ash replacement, the 400% dosage specimens exhibit more shrinkage after 28 days than other mixes.

It is proposed that this increased later autogenous shrinkage at the highest dosage examined may be due to effects of the initial hydration acceleration on the developing microstructure. Cement pastes have been shown to have a coarser microstructure and higher percentage of larger pores in pastes when hydration has been accelerated by addition of sodium hydroxide (NaOH) [24]. A coarser microstructure and increased larger pore volume has been shown to increase autogenous shrinkage [25]. In Garci Juenger's research [24], alkali-induced acceleration comparable to that seen in Figs. 1–6 led to microstructural differences and to increased specimen shrinkage after 40 days. Pastes in this research, accelerated by lithium nitrate addition rather than

sodium hydroxide, behaved similarly. However, it is worth noting that low alkali Cement 1, where early hydration was most accelerated by lithium nitrate addition, shows the least effect of lithium addition on autogenous shrinkage. Thus, further research is necessary to completely understand the relationships between hydration, microstructure development, and autogenous shrinkage with the addition of lithium nitrate.

The increased shrinkage in the 400% LiNO_3 dosage specimens for all cements is significant because autogenous shrinkage, occurring after final set, can induce tensile stresses in concrete. Higher tensile stresses can cause cracking, and may also increase the likelihood of localized ASR expansive forces causing cracking. Prior shrinkage research with lithium admixtures has considered dosages at or just below the recommended (i.e., 100% and 75%, respectively), [26]. Further work, including analytical characterization, is necessary to understand the significance of this increased shrinkage on concrete performance.

The cause of the initial autogenous expansion in the specimens with higher lithium dosages is not known. Re-absorption of bleed water is known to cause such expansions during autogenous shrinkage testing, but no lithium effect on bleed water was observed in this work [27]. Another possible cause of the initial expansions may be the early formation of large-sized crystals of calcium hydroxide suggested by Baroghel-Bouny et al. [28]. The increased rate of nucleation of calcium-containing products caused by lithium may lead to calcium hydroxide crystals exerting localized expansive forces within the developing microstructure. Further research is necessary to better understand this behavior.

4. Conclusions

The influence of lithium nitrate admixture on hydration behavior of five cements was investigated through calorimetry, setting time, and chemical and autogenous shrinkage measurements. The cements were selected to examine the influence of variations in cement composition. The following observations may be made:

- The LiNO_3 admixture accelerates the hydration of the tricalcium silicate (C_3S) and tricalcium aluminate (C_3A) components of cement, generating more early heat than control mixes and experiencing generally greater chemical shrinkage in the first 24 h. This acceleration relative to the control mixes was observed in the calorimetry data for all cements tested, and at all dosages. Importantly, lower alkali cements, which are more likely to be specified in applications where ASR is a concern, appear more susceptible to this acceleration. Although the lithium sensitivity of a cement likely depends on more variables than just alkali content, alkali content is likely a key factor.
- It is proposed that the presence of the Li^+ alkali ion likely accelerates early C_3S hydration by reducing the solubility of calcium-containing hydration products in the saturated mix water, thereby advancing nucleation. Early acceleration of the C_3A component may be due to lithium promoting its dissolution. Comparison of calorimetry results for cements of various alkali contents suggests that acceleration effects of lithium, sodium, and potassium are additive. Addition of lithium to low alkali cements causes a larger relative increase

in the combined $[\text{Li}^+ + \text{Na}^+ + \text{K}^+]$ concentration, causing greater acceleration than in high alkali cements.

- This acceleration, and the increase in early heat generation, may be harmful in some concrete applications where high temperatures are a concern. However, calorimetry results also indicate that the inclusion of Class F fly ash at 20% by weight replacement of cement appears to diminish these possibly negative effects of LiNO_3 on early-age heat generation. Since Class F fly ash has ASR-mitigating effects of its own, its use in applications where lithium nitrate is specified is appropriate.
- While the use of lithium nitrate accelerates early hydration, calorimetry and chemical shrinkage data suggest that hydration may be retarded after 1 day by the presence of this chemical admixture.
- The times of initial and final setting of paste specimens were only affected in the lowest alkali cement tested. In this low alkali cement ($\text{Na}_2\text{O}_e = 0.295\%$), initial and final set times were decreased by 15% and 22%, respectively, by the recommended dosage. However, no indication of early stiffening or flash-set was apparent at any dosage, and the reduction in set time for the low alkali cement is likely manageable in the field.
- While higher LiNO_3 dosages appeared to cause initial expansion in some sealed paste specimens, greater autogenous shrinkage was apparent in the 400%-lithium pastes after 40 days, for all cements examined. This shrinkage may be due to the coarser microstructure with higher percentage of large pores caused by hydration acceleration. Further research, including analytical characterization, is needed to better understand this behavior and the potential implications on overall performance.

Overall, the results suggest that lithium nitrate admixtures are likely innocuous when used at recommended dosages rates, for most cements. However, additional testing may be warranted to examine early setting, heat evolution, and shrinkage, for critical applications, particularly with low alkali cements. In general, however, variations in behaviour were greater between the different cements than with increasing lithium nitrate admixture dosage for a particular cement.

Acknowledgements

This research results from Innovative Pavement Research Foundation (IPRF) and the Federal Aviation Administration (FAA) support of Project 04-06. The authors also acknowledge Heidelberg Technology Center for technical assistance, as well as David Stokes of FMC Lithium, Prasad Rangaraju of Clemson University and Dale Bentz of NIST for their insightful comments. The contributions of Richard L. Boudreau and Viswanath Dokka of Accura Engineering and Consulting Services, Inc. are also acknowledged. The statements made here do not necessarily represent the views of the sponsors.

References

- [1] T.E. Stanton, Expansion of concrete through reaction between cement and aggregate, *Proceedings of the American Society of Civil Engineers* 66 (10) (1940) 1781–1811.
- [2] A. Carse, Review of the present condition of the Lucinda Bulk Sugar Terminal at Lucinda in North Queensland Australia, *Proceedings of the 12th International Conference on Alkali–Aggregate Reaction in Concrete*, Beijing, 2004, pp. 1025–1034.
- [3] K.J. Folliard, M.D. Thomas, K.E. Kurtis, Guidelines for the use of lithium to mitigate or prevent ASR, FHWA Report: FHWA-RD-03-047, July 2003.
- [4] Fu Pei-xing, Jun-min Wang, Alkali reactivity of aggregates and AAR-affected concrete structures in Beijing, *Proceedings of the 12th International Conference on Alkali–Aggregate Reaction in Concrete*, Beijing, 2004, pp. 1055–1061.
- [5] P. Rangaraju, J. Olek, Potential for acceleration of ASR in the presence of pavement deicing chemicals, IPFR Project 01-G-002-03-9, 2005.
- [6] W.J. McCoy, A.G. Caldwell, New approach to inhibiting alkali–aggregate expansion, *ACI Journal* 22 (9) (1951) 693–705.
- [7] M. Thomas, R. Hooper, D. Stokes, Use of lithium-containing compounds to control expansion in concrete due to alkali–silica reaction, *Proceedings of the 11th International Conference on Alkali–Aggregate Reaction in Concrete*, Centre de Recherche Interuniversitaire sur le Beton (CRIB), Canada, 2000.
- [8] B. Durand, More results about the use of lithium salts and mineral admixtures to inhibit ASR in concrete, *Proceedings of the 11th International Conference on Alkali–Aggregate Reaction (ICAAAR)*, Quebec, Canada, June 11–16 2000, pp. 623–632.
- [9] C.L. Collins, J.H. Ideker, K.E. Kurtis, Laser scanning confocal microscopy for in situ monitoring of alkali–silica reaction, *Journal of Microscopy* 213 (Feb 2004) 149–157.
- [10] H. Wang, D.B. Stokes, Compatibility of lithium-based admixtures with other concrete admixtures, *Proceedings of the 10th International Conference on Alkali–Aggregate Reaction (ICAAAR)*, Melbourne, Australia, August 18–23, 1996, pp. 884–891.
- [11] Standard Test Method for Chemical Shrinkage of Hydraulic Cement Paste. ASTM Designation C 1608-05, American Society for Testing and Materials, West Conshohocken, PA, 2005.
- [12] Standard Test Method for Time of Setting of Hydraulic Cement by Vicat Needle. ASTM Designation C 191-04b, American Society for Testing and Materials, West Conshohocken, PA, 2004.
- [13] Standard Practice for Mechanical Mixing of Hydraulic Cement Pastes and Mortars of Plastic Consistency. ASTM Designation C 305-99, American Society for Testing and Materials, West Conshohocken, PA, 1999.
- [14] O. Mejlhede Jensen, P. Freiesleben Hansen, A dilatometer for measuring autogenous deformation in hardening portland cement paste, *Materials and Structures* 28 (1995) 407–409.
- [15] Dale P. Bentz, Lithium, potassium, and sodium additions to cement pastes, *Advances in Cement Research* 18 (2006) 65–70.
- [16] Inam Jawed, Jan Skalný, Alkalies in cement: a review, *Cement and Concrete Research* 8 (1978) 37–52.
- [17] I. Odler, H. Dorr, Early hydration of tricalcium silicate II the induction period, *Cement and Concrete Research* 9 (May 1979) 277–284.
- [18] Peter C. Hewlett, *Lea's Chemistry of Cement and Concrete*, 4th ed., Arnold, London, 1998, pp. 874–875.
- [19] S. Diamond, Unique response of LiNO_3 as an alkali silica reaction-preventive admixture, *Cement and Concrete Research* 29 (1999) 1271–1275.
- [20] J. Gajda, Development of a cement to inhibit alkali–silica reactivity, PCA Research and Development Bulletin RD 115T, Portland Cement Association, Skokie, Illinois, 1996.
- [21] X. Mo, Laboratory study of LiOH in inhibiting alkali–silica reaction at 20 °C: a contribution, *Cement and Concrete Research* 35 (March 2005) 499–504.
- [22] M.D.A. Thomas, D. Stokes, T. Rodgers, The effect of lithium-based admixtures on the properties of concrete, in: V.M. Malhotra (Ed.), 7th CANMET/ACI International Conference on Superplasticizers and other Chemical Admixtures in Concrete, SP-217, American Concrete Institute, Farmington Hills, Michigan, September 2003.
- [23] J. Weiss, P. Lura, S. Gaurav, Measurement of volume change in cementitious materials at early ages: review of testing protocols and interpretation of results, *Transportation Research Record, Concrete Materials* 1979 (2006) 21–29.
- [24] M.C. Garci Juenger, H.M. Jennings, Effects of high alkalinity on cement pastes, *ACI Materials Journal* 98 (3) (May–June, 2001) 251.

- [25] Shin-ichi Igarashi, A. Watanabe, M. Kawamura, Evaluation on capillary pore size characteristics in high-strength concrete at early ages, *Cement and Concrete Research* 35 (2005) 513–519.
- [26] D.S. Lane, Laboratory investigation of lithium-bearing compounds for use in concrete, VTRC 02-R16, Virginia Transportation Research Council, Commonwealth of Virginia, June 2002.
- [27] R.L. Boudreau, M. Millard, K. Kurtis, V. Dokka, Lithium admixtures (LiNO_3) and early age concrete properties, IPRF-01-G-002-04-6, Innovative Pavement Research Foundation, November 2006 also at http://iprf.org/products/Publication%20Version_Proj%2004-6.pdf.
- [28] V. Baroghel-Bouny, P. Mounanga, A. Loukili, A. Khelidj, From chemical and microstructural evolution of cement pastes to the development of autogenous deformations, American Concrete Institute Autogenous Deformation of Concrete Symposium, Oct 2002.